

Stopping powers and energy loss of Mylar, Kapton, Havar, and Ni for 10 $Z = 3 - 17$ ions in the energy range 0.2–2.1 MeV/amu

J. Räsänen and E. Rauhala

Accelerator Laboratory, University of Helsinki, Hämementie 100, SF-00550 Helsinki, Finland

(Received 2 October 1989)

Stopping powers of Mylar, Kapton, Havar, and nickel for 0.27–1.94 MeV/amu ^{11}B ions, 1.27–2.07 MeV/amu ^{12}C , 0.58–1.80 MeV/amu ^{14}N , and for 0.67–1.78 MeV/amu ^{16}O ions have been determined. Energy loss and stopping powers of Mylar were measured for ^{27}Al , ^{28}Si , ^{31}P , ^{32}S , and ^{35}Cl ions having energies between 7.6 and 24.6 MeV. Direct beam exposure of the foils was avoided by using a modified transmission geometry. Proton-energy loss, in the same geometry and at exactly the spot of the heavy-ion beam on the foils, was taken as a measure of foil thickness. The present data are brought together with our recent measurements of the stopping powers of the materials in this study for ^7Li , ^{11}B , ^{12}C , ^{14}N , and ^{16}O ions. The experimental stopping powers are compared with predictions of two semiempirical scaling models, used in conjunction with Bragg's additivity rule, and with the stopping powers obtained by the TRIM-89 computer code. Comparisons have also been performed with the scanty experimental data in the literature. The systematics and the deviations of the stopping powers from the calculated predictions are discussed.

I. INTRODUCTION

The stopping of ions traversing matter has been of considerable interest in the past decades both from a theoretical and from an experimental point of view. The knowledge of stopping powers is of the utmost importance in applications involving the probing of materials with beams of energetic ions. Experimental data are necessary in the development of the theoretical approaches as well as in applications where the slowing down of ions must be known with good accuracy.

We have recently performed a series of experiments^{1–4} to determine the stopping powers of ^7Li , ^{12}C , ^{14}N , and ^{16}O ions in the simple organic compounds Mylar and Kapton. A more complex metallic-composite material, Havar, has also been included together with an elemental material, nickel. The present study extends these experiments both to new ions and higher energies. Looking at all these data together, new systematic behavior was observed. The present experiments were performed in the energy interval of 3.0–28.5 MeV.

Since accurate experimental energy-loss values in the use of the heavy-ion elastic-recoil detection analysis (ERDA) are needed, the energy loss of ^{27}Al , ^{28}Si , ^{31}P , ^{32}S , and ^{35}Cl ions between 7.6 and 16.9 MeV in 3.26- μm -thick Mylar, in addition to the stopping powers in the range 10.4–24.6 MeV, were determined.

Very little previous experimental data for ions used in the present study may be found in the literature. In addition to works cited in the present study, these data have been presented in our previous studies^{1–4} and in references therein.

The experimental stopping powers are compared with the scaled proton stopping powers calculated by two semiempirical models and the TRIM-89 computer code. The first model by Ziegler,⁵ (abbreviated as Z-80) is based on the Z_1 -dependent parametrizations of the heavy-ion

effective charge. It should be noted that in Z-80 a separate parametrization for the effective charge of ^7Li ions is given. This leads to scaling different from that of all other ions heavier than ^7Li . The second model is based on the Brandt-Kitagawa theory.⁶ It was presented by Ziegler, Biersack, and Littmark (ZBL-85).⁷ It includes a refined treatment of effective charges and considerations of relative velocities between the ion and the Fermi velocity of electrons in a solid, as well as nuclear shielding in close collisions. The TRIM-89 computer code (version 5.3)⁸ uses the theoretical basis of the latter semiempirical model. In addition, however, the correction due to the chemical bonding in compounds like Mylar and Kapton can be accounted for.⁹

II. EXPERIMENTAL PROCEDURE

The ion beams were supplied by the 5-MV tandem accelerator EGP-10-II of the Accelerator Laboratory of the University of Helsinki. The energy calibration of the beam-analyzing magnet was based on the resonances at $E_{\text{lab}}(^{15}\text{N}) = 6393.6 \pm 1.3$, $13\,356 \pm 4$, $18\,009 \pm 45$, and $24\,409 \pm 45$ keV in the reaction $^1\text{H}(^{15}\text{N}, \alpha\gamma)^{12}\text{C}$ and the very thin H contamination on the surface of an Au target. A standard silicon surface-barrier detector (100 μm , 50 mm^2) was used.

The charge states of the ions used are given in Table I. The energy interval of the experiments for each of the ions was limited at the high-energy end by the highest charge state of practical use and the terminal voltage available from the accelerator. The energy interval of our previous experiments or the ion range of the order of the foil thickness, defined the low-energy end of the energy interval in our present measurements.

The experimental arrangement is schematically illustrated in Fig. 1. A thick gold target was used to scatter the ions from the accelerator. The sample foil was inter-

TABLE I. Characteristics of the ion beams used in the present study.

| Ion | Charge state | Energy region (MeV) |
|------------------|--------------|---------------------|
| ^{11}B | +2 | 4.5–11.0 |
| | +3 | 12.0–19.0 |
| | +4 | 20.0–23.0 |
| ^{12}C | +4 | 21.0–22.0 |
| | +5 | 23.0–27.0 |
| ^{14}N | +5 | 21.0–28.0 |
| ^{16}O | +5 | 20.0–28.0 |
| | +6 | 29.0–33.0 |
| ^{27}Al | +3 | 10.0–16.0 |
| | +4 | 17.0–21.0 |
| ^{28}Si | +4 | 13.0–24.0 |
| | +5 | 25.0–28.0 |
| | +6 | 29.0–33.0 |
| ^{31}P | +4 | 15.0–24.0 |
| | +5 | 25.0–27.0 |
| | +6 | 28.0–32.0 |
| ^{32}S | +4 | 14.0–22.0 |
| | +5 | 23.0–28.0 |
| | +6 | 29.0–32.0 |
| ^{35}Cl | +5 | 19.0–28.0 |
| | +6 | 29.0–33.0 |

posed into the scattered ion beam in front of the detector. The most probable energy loss of the ions transmitted through the foil was obtained from the reduction of the ion-energy scattering from the surface layer of the gold target. By this procedure, a sufficiently low-intensity ion flux was obtained and problems caused by heat and charge accumulation on the foil were avoided. Direct beam exposure of the foils on the other hand, would significantly modify the properties of the foils.¹

To extract stopping powers from the energy-loss data, the areal densities of the foils were determined from the energy-loss of 2.0–4.0 MeV protons in the foils. Proton

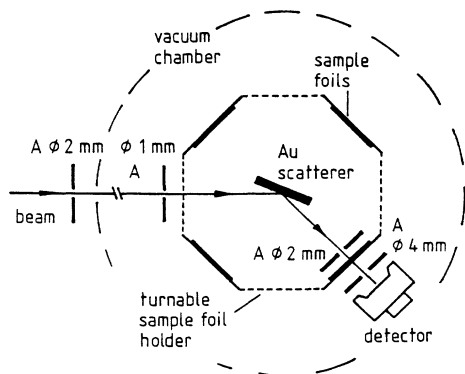


FIG. 1. A schematic diagram of the experimental setup. Collimating slits and apertures with diameters " ϕ " are denoted by "A."

energy loss was measured using the same geometry and at exactly the same spot on the foils as the heavier-ion energy loss. Contrary to other methods of areal-density measurement (e.g., weighing), where a density over a larger sample area is averaged, the effective local areal density obtained by this method is in terms of the proton stopping powers.¹⁰ This procedure has been investigated in detail, as were the proton stopping powers determined in our previous study.¹¹ In this previous study, the proton stopping powers at 2–4 MeV were observed to agree within 3% with the semiempirical predictions.¹⁰ A small correction to the semiempirical predictions has been taken into account according to our proton-stopping-power data.

III. RESULTS

The stopping power at the mean ion energy E_{av} in the foil is obtained by dividing the energy-loss ΔE by the foil areal density $N\Delta x$ (N —atomic density, Δx —foil thickness). The nominal specific gravities used in unit conversions and some properties of the composite foil materials (as given by the manufacturers) are presented in Table II.

To account for the nonlinear dependence of the stopping powers on ion energy, a small correction^{12,3} to the mean energy E_{av} was applied. As a result, the stopping power $S=dE/dx$ (differential energy loss per unit path length) is taken as $\Delta E/\Delta x$ at an effective ion energy E_{eff} . The correction procedure for E_{eff} is valid only when $\Delta E < E_{av}$. In the case of large energy-loss values, the

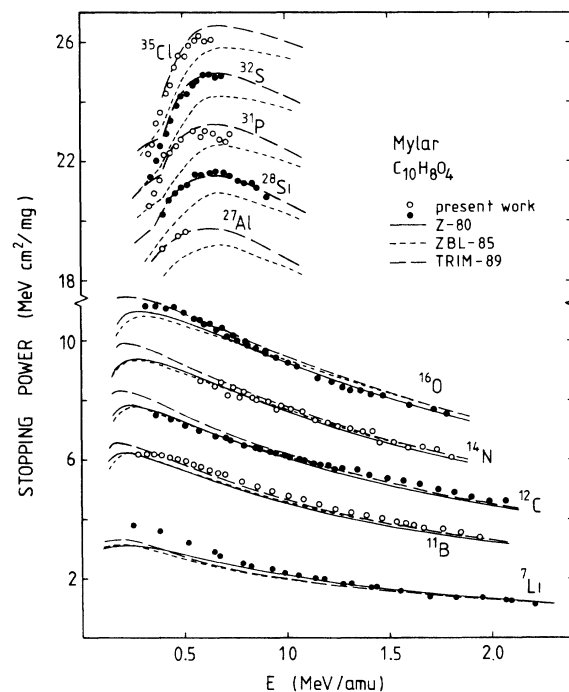


FIG. 2. Stopping powers of Mylar for ^7Li , ^{11}B , ^{12}C , ^{14}N , ^{16}O , ^{27}Al , ^{28}Si , ^{31}P , ^{32}S , and ^{35}Cl ions. The data points comprise both our new data and the data from our previous studies. The curves represent the stopping powers as predicted by semiempirical scaling models.

TABLE II. Nominal compositions, average atomic weights, and specific gravities of Mylar, Kapton, and Havar.

| Foil | Element | Concentration (at. %) |
|---|---------|-----------------------|
| Mylar ($C_{10}H_8O_4$) _x $M=8.73$ amu $\rho=1.39$ g/cm ³ | H | 36.4 |
| | C | 45.4 |
| | O | 18.2 |
| Kapton ($C_{22}H_{10}O_5N_2$) _x $M=9.79$ amu $\rho=1.42$ g/cm ³ | H | 25.6 |
| | C | 56.4 |
| | N | 5.1 |
| | O | 12.8 |
| Havar $M=57.6$ amu $\rho=8.30$ g/cm ³ | Be | 0.3 |
| | C | 1.0 |
| | Cr | 22.2 |
| | Mn | 1.7 |
| | Fe | 18.1 |
| | Co | 41.6 |
| | Ni | 12.8 |
| | Mo | 1.4 |
| | W | 0.9 |

TABLE III. The stopping powers of ¹¹B ions in Mylar, Kapton, Havar, and nickel.

| E (MeV) | Mylar | Stopping power (MeV cm ² /mg) | | | | Havar | E (MeV) | Nickel |
|-----------|-------|--|--------|-----------|------|-------|-----------|--------|
| | | E (MeV) | Kapton | E (MeV) | | | | |
| 2.99 | 6.16 | 6.92 | 5.47 | 4.94 | 2.93 | 6.92 | 2.81 | |
| 3.40 | 6.18 | 7.88 | 5.30 | 5.34 | 2.94 | 7.73 | 2.83 | |
| 3.81 | 6.20 | 8.84 | 5.10 | 5.76 | 2.94 | 8.62 | 2.79 | |
| 4.22 | 6.16 | 9.76 | 4.97 | 6.17 | 2.95 | 9.47 | 2.76 | |
| 4.66 | 6.09 | 10.67 | 4.83 | 7.02 | 2.93 | 10.36 | 2.72 | |
| 5.09 | 6.05 | 11.60 | 4.67 | 7.91 | 2.89 | 11.25 | 2.66 | |
| 5.51 | 5.96 | 12.52 | 4.51 | 8.77 | 2.85 | 12.13 | 2.62 | |
| 5.96 | 5.83 | 13.43 | 4.37 | 9.68 | 2.77 | 13.05 | 2.54 | |
| 6.37 | 5.78 | 14.33 | 4.24 | 10.55 | 2.72 | 13.93 | 2.49 | |
| 6.81 | 5.67 | 15.20 | 4.15 | 11.43 | 2.65 | 14.81 | 2.44 | |
| 7.24 | 5.56 | 16.18 | 4.01 | 12.29 | 2.60 | 15.25 | 2.41 | |
| 7.68 | 5.45 | 17.28 | 3.88 | 13.18 | 2.52 | 15.71 | 2.38 | |
| 8.55 | 5.25 | 18.31 | 3.76 | 14.05 | 2.46 | 16.32 | 2.33 | |
| 9.40 | 5.10 | 19.34 | 3.65 | 14.92 | 2.40 | 17.33 | 2.30 | |
| 10.24 | 4.97 | 20.37 | 3.55 | 15.78 | 2.35 | 18.39 | 2.24 | |
| 11.09 | 4.79 | | | 16.50 | 2.29 | 19.46 | 2.15 | |
| 11.93 | 4.70 | | | 17.36 | 2.24 | | | |
| 12.78 | 4.52 | | | 18.39 | 2.17 | | | |
| 13.63 | 4.39 | | | 19.41 | 2.13 | | | |
| 14.48 | 4.26 | | | 20.43 | 2.07 | | | |
| 15.30 | 4.17 | | | | | | | |
| 16.14 | 4.06 | | | | | | | |
| 16.98 | 3.95 | | | | | | | |
| 17.35 | 3.89 | | | | | | | |
| 17.83 | 3.82 | | | | | | | |
| 18.36 | 3.74 | | | | | | | |
| 19.33 | 3.72 | | | | | | | |
| 20.33 | 3.61 | | | | | | | |
| 21.34 | 3.42 | | | | | | | |

TABLE IV. The stopping powers of ^{12}C ions in Mylar, Kapton, Havar, and nickel.

| E (MeV) | Mylar | E (MeV) | Stopping power (MeV cm ² /mg) | | Havar | E (MeV) | Nickel |
|-----------|-------|-----------|--|-----------|-------|-----------|--------|
| | | | Kapton | E (MeV) | | | |
| 16.85 | 5.53 | 15.18 | 5.65 | 17.44 | 3.31 | 15.89 | 3.24 |
| 17.84 | 5.40 | 16.26 | 5.45 | 18.37 | 3.23 | 16.84 | 3.18 |
| 18.83 | 5.31 | 17.31 | 5.30 | 19.50 | 3.15 | 18.02 | 3.11 |
| 19.82 | 5.21 | 18.22 | 5.23 | 20.54 | 3.07 | 19.10 | 3.02 |
| 20.84 | 5.03 | 19.39 | 5.06 | 21.54 | 3.03 | 20.15 | 2.97 |
| 21.82 | 4.95 | 20.39 | 4.98 | 22.56 | 2.96 | 21.19 | 2.92 |
| 22.84 | 4.77 | 21.45 | 4.81 | 23.54 | 2.94 | 22.25 | 2.85 |
| 23.85 | 4.63 | 22.51 | 4.65 | | | | |
| 24.81 | 4.65 | 23.49 | 4.64 | | | | |

stopping powers based on only experimental data can not be extracted without any assumption about the stopping-power curve.

The new stopping powers of Mylar, Kapton, Havar, and nickel for ^{11}B , ^{12}C , ^{14}N , and ^{16}O ions as a function of effective ion energy $E = E_{\text{eff}}$ are presented in Tables III–VI and of Mylar for ^{27}Al , ^{28}Si , ^{31}P , ^{32}S , and ^{35}Cl ions in Table VII. The data are assigned an uncertainty of $\pm 4\%$. This includes the possible 3% error arising from the determination of the foil thickness by the proton-energy-loss measurements and the uncertainties in the

measurement of ΔE . When the condition $\Delta E < E_{\text{av}}$ is not fulfilled, no stopping powers were calculated and the energy-loss values are given. The new energy-loss data for ^{11}B in 8.90- μm Kapton, 2.12- μm Havar, and 2.74- μm nickel and for heavier ions ^{27}Al , ^{28}Si , ^{31}P , ^{32}S , and ^{35}Cl in 3.26- μm Mylar, as a function of incident-ion energy on the sample foil, are presented in Tables VIII and IX. To bring together our relevant previous data and to illustrate the overall behavior of the stopping powers, as well as to present comparisons with the theoretical models, the stopping powers are plotted in Figs. 2–5.

TABLE V. The stopping powers of ^{14}N ions in Mylar, Kapton, Havar, and nickel.

| E (MeV) | Mylar | E (MeV) | Stopping power (MeV cm ² /mg) | | Havar | E (MeV) | Nickel |
|-----------|-------------------|-----------|--|-----------|-------------------|-----------|-------------------|
| | | | Kapton | E (MeV) | | | |
| 8.17 | 8.65 ^a | 10.64 | 8.20 | 8.09 | 4.43 | 10.65 | 4.18 |
| 9.05 | 8.46 ^a | 11.57 | 7.99 | 8.12 | 4.40 ^a | 11.41 | 4.10 ^a |
| 9.50 | 8.59 | 12.45 | 7.86 | 8.88 | 4.43 | 11.44 | 4.17 |
| 9.99 | 8.15 ^a | 13.35 | 7.69 | 8.89 | 4.41 ^a | 12.24 | 4.17 |
| 10.32 | 8.43 | 14.24 | 7.54 | 9.70 | 4.38 ^a | 13.05 | 4.15 |
| 10.79 | 8.09 ^a | 15.06 | 7.45 | 9.71 | 4.39 | 13.89 | 4.11 |
| 11.11 | 8.28 | 16.03 | 7.31 | 10.49 | 4.38 ^a | 14.56 | 4.08 |
| 11.57 | 8.09 ^a | 17.00 | 7.16 | 10.50 | 4.38 | 15.51 | 4.02 |
| 11.95 | 8.01 | 18.29 | 7.39 | 11.25 | 4.41 ^a | 16.58 | 3.94 |
| 12.73 | 7.96 | 19.28 | 6.83 | 11.31 | 4.35 | 17.67 | 3.86 |
| 13.32 | 7.66 ^a | 20.35 | 6.65 | 12.13 | 4.31 | 18.72 | 3.80 |
| 13.54 | 7.80 | 21.30 | 6.66 | 12.95 | 4.26 | 19.68 | 3.80 |
| 14.34 | 7.70 | 22.30 | 6.61 | 12.97 | 4.24 ^a | 20.79 | 3.70 |
| 15.13 | 7.61 | 23.38 | 6.40 | 13.05 | 4.18 | 21.80 | 3.67 |
| 15.96 | 7.33 | | | 13.87 | 4.13 | | |
| 16.75 | 7.26 | | | 14.66 | 4.12 | | |
| 17.55 | 7.13 | | | 15.47 | 4.08 | | |
| 18.28 | 7.05 | | | 16.34 | 4.03 | | |
| 19.15 | 6.94 | | | 17.12 | 3.97 | | |
| 19.89 | 6.96 | | | 17.45 | 3.98 | | |
| 20.28 | 6.58 | | | 17.89 | 3.97 | | |
| 21.25 | 6.60 | | | 18.51 | 3.88 | | |
| 22.26 | 6.41 | | | 19.52 | 3.83 | | |
| 23.20 | 6.45 | | | 20.58 | 3.73 | | |
| 24.19 | 6.35 | | | 21.52 | 3.75 | | |
| 25.22 | 6.09 | | | 22.53 | 3.69 | | |
| | | | | 23.60 | 3.58 | | |

^aEnergy loss data from Ref. 1.

TABLE VI. The stopping powers of ^{16}O ions in Mylar, Kapton, Havar, and nickel.

| E (MeV) | Mylar | Stopping power (MeV cm ² /mg) | | | | | |
|-----------|-------|--|--------|-----------|-------|-----------|--------|
| | | E (MeV) | Kapton | E (MeV) | Havar | E (MeV) | Nickel |
| 19.53 | 8.62 | 15.42 | 9.20 | 10.82 | 5.10 | 15.12 | 4.95 |
| 20.25 | 8.43 | 16.27 | 8.98 | 11.58 | 5.09 | 15.81 | 4.93 |
| 21.01 | 8.32 | 17.06 | 8.90 | 12.36 | 5.06 | 16.64 | 4.88 |
| 21.68 | 8.32 | 17.92 | 8.75 | 13.10 | 5.07 | 17.31 | 4.89 |
| 22.52 | 8.19 | 18.75 | 8.64 | 13.88 | 5.04 | 18.13 | 4.89 |
| 23.55 | 8.15 | 19.14 | 8.56 | 14.66 | 5.00 | 19.30 | 4.81 |
| 25.54 | 7.81 | 21.18 | 8.36 | 15.49 | 4.92 | 21.37 | 4.70 |
| 27.48 | 7.68 | 23.22 | 8.13 | 16.24 | 4.91 | 23.46 | 4.58 |
| 28.48 | 7.53 | 25.25 | 7.92 | 17.01 | 4.89 | 24.49 | 4.53 |
| | | 26.27 | 7.81 | 17.71 | 4.83 | | |
| | | | | 18.58 | 4.80 | | |
| | | | | 19.48 | 4.75 | | |
| | | | | 20.14 | 4.72 | | |
| | | | | 21.62 | 4.64 | | |
| | | | | 23.62 | 4.53 | | |
| | | | | 25.67 | 4.38 | | |
| | | | | 26.63 | 4.37 | | |

TABLE VII. The stopping powers of ^{27}Al , ^{28}Si , ^{31}P , ^{32}S , and ^{35}Cl ions in Mylar.

| E (MeV) | ^{27}Al | Stopping power (MeV cm ² /mg) | | | | | | | |
|-----------|------------------|--|------------------|-----------|-----------------|-----------|-----------------|-----------|------------------|
| | | E (MeV) | ^{28}Si | E (MeV) | ^{31}P | E (MeV) | ^{32}S | E (MeV) | ^{35}Cl |
| 11.01 | 19.04 | 10.66 | 20.20 | 10.36 | 20.48 | 10.94 | 21.47 | 11.43 | 22.26 |
| 12.81 | 19.45 | 11.47 | 20.65 | 11.16 | 20.91 | 11.70 | 22.01 | 12.26 | 22.59 |
| 13.71 | 19.66 | 12.34 | 20.91 | 11.93 | 21.47 | 12.48 | 22.52 | 12.98 | 23.28 |
| | | 13.23 | 21.10 | 12.63 | 22.22 | 13.30 | 22.91 | 13.79 | 23.64 |
| | | 14.15 | 21.19 | 13.56 | 22.26 | 14.11 | 23.36 | 14.52 | 24.29 |
| | | 15.00 | 21.56 | 14.42 | 22.52 | 14.88 | 23.86 | 15.34 | 24.56 |
| | | 15.96 | 21.53 | 15.25 | 22.70 | 15.73 | 24.18 | 16.11 | 25.17 |
| | | 16.88 | 21.60 | 17.14 | 23.00 | 16.63 | 24.25 | 16.92 | 25.54 |
| | | 17.82 | 21.66 | 18.15 | 22.82 | 17.47 | 24.55 | 17.86 | 25.51 |
| | | 18.78 | 21.60 | 19.03 | 23.00 | 18.36 | 24.70 | 18.66 | 25.88 |
| | | 19.75 | 21.50 | 20.00 | 22.93 | 19.23 | 24.91 | 19.53 | 26.05 |
| | | 20.73 | 21.32 | 21.00 | 22.70 | 20.15 | 24.95 | 20.40 | 26.22 |
| | | 21.68 | 21.25 | 21.93 | 22.65 | 21.10 | 24.83 | 21.39 | 26.01 |
| | | 22.60 | 21.27 | 22.76 | 22.95 | 22.02 | 24.88 | 22.29 | 26.09 |
| | | 23.59 | 21.10 | | | | | | |
| | | 24.58 | 20.78 | | | | | | |

TABLE VIII. The energy loss ΔE of ^{11}B ions in Havar, Kapton, and nickel.

| E (MeV) | ΔE (MeV) | | | | | |
|-----------|-----------------------|-----------|-----------------------|-----------|-----------------------|-----------|
| | Kapton | | Nickel | | Havar | |
| | (8.90 μm) | E (MeV) | (2.74 μm) | E (MeV) | (2.12 μm) | E (MeV) |
| 8.52 | 7.16 | 4.87 | 4.32 | 6.90 | 6.22 | |
| 8.93 | 7.12 | 5.28 | 4.51 | 7.30 | 6.38 | |
| 9.74 | 7.12 | 5.68 | 4.68 | 7.71 | 6.54 | |
| | | 6.09 | 4.81 | 8.12 | 6.67 | |
| | | 6.49 | 4.92 | 8.52 | 6.78 | |
| | | 6.90 | 4.99 | 8.93 | 6.87 | |
| | | 7.30 | 5.11 | 9.74 | 6.85 | |
| | | 7.71 | 5.15 | | | |

TABLE IX. The energy loss ΔE of ^{27}Al , ^{28}Si , ^{31}P , ^{32}S , and ^{35}Cl ions in 3.26- μm -thick Mylar foil.

| E (MeV) | ^{27}Al | E (MeV) | ^{28}Si | ΔE (MeV) | | E (MeV) | ^{32}S | E (MeV) | ^{35}Cl |
|-----------|------------------|-----------|------------------|------------------|-----------------|-----------|-----------------|-----------|------------------|
| | | | | E (MeV) | ^{31}P | | | | |
| 7.77 | 5.50 | 7.62 | 5.52 | 7.74 | 5.48 | 7.60 | 5.42 | 9.72 | 6.29 |
| 8.37 | 5.83 | 8.21 | 5.86 | 8.30 | 5.79 | 8.14 | 5.73 | 10.23 | 6.54 |
| 8.97 | 6.14 | 8.79 | 6.21 | 8.85 | 6.07 | 8.68 | 6.04 | 10.74 | 6.83 |
| 9.40 | 6.35 | 9.38 | 6.54 | 9.40 | 6.40 | 9.22 | 6.35 | 11.26 | 7.03 |
| 10.16 | 6.69 | 9.97 | 6.88 | 9.96 | 6.70 | 9.77 | 6.65 | 11.77 | 7.29 |
| 11.07 | 7.15 | 10.55 | 7.12 | 10.51 | 6.94 | 10.31 | 6.93 | 12.28 | 7.53 |
| 12.00 | 7.59 | 11.14 | 7.44 | 11.06 | 7.19 | 10.85 | 7.22 | 12.79 | 7.76 |
| 12.92 | 7.89 | 11.73 | 7.67 | 11.62 | 7.46 | 11.40 | 7.51 | 13.30 | 7.98 |
| 13.84 | 8.19 | 12.31 | 7.05 | 12.17 | 7.65 | 11.94 | 7.80 | 13.81 | 8.19 |
| 14.76 | 8.43 | 12.90 | 8.09 | 12.74 | 7.92 | 12.48 | 7.94 | 14.33 | 8.41 |
| | | 13.48 | 8.35 | 13.48 | 8.16 | 13.02 | 8.19 | 14.84 | 8.64 |
| | | 14.07 | 8.51 | 14.59 | 8.66 | 13.56 | 8.40 | 15.33 | 8.97 |
| | | 14.66 | 8.71 | | | 14.10 | 8.63 | 15.86 | 9.08 |
| | | 15.24 | 8.74 | | | 14.60 | 8.84 | 16.29 | 9.34 |
| | | 15.82 | 8.95 | | | 15.32 | 9.05 | 16.88 | 9.55 |
| | | 16.42 | 9.15 | | | | | | |

IV. DISCUSSION

The heavy-ion stopping powers based on the Ziegler parameters for scaling proton stopping powers (Z-80),⁵ those based on the Brandt-Kitagawa theory (ZBL-85),^{6,7} and stopping powers calculated by the TRIM-89 computer code⁸ are presented together with all our experimental data in Figs. 2–5. In the composite foil cases the Bragg's additivity rule has been used in conjunction with the Z-80 and ZBL-85 models. In the curves referred to as TRIM-89, a correction⁹ to account for the stopping-power contribution of the chemical bonds of the compounds Mylar and Kapton has been applied.

In the light-compound-foil cases of Mylar and Kapton the experimental stopping powers are in general best fitted by the TRIM-89 curves. Good consistency between the TRIM-89 calculations and the data may be found for all ions except for ^7Li in both of the foils, and for ^{12}C below 1.0 MeV/amu and ^{16}O above 1.0 MeV/amu in My-

lar. Discrepancies of 15%, 5%, and 4% at maximum, respectively, are observed. The experimental stopping powers for ^{11}B ions are slightly larger than the calculated values. The predictions of the Z-80 and ZBL-85 models generally underestimate the stopping powers. For ^7Li ions, the separate scaling of Z-80 is more successful than the TRIM-89 calculations or the ZBL-85 model.

In the case of the metallic foils of Ni and Havar, good agreement between experimental stopping and the calculated predictions is observed for ^{14}N and ^{16}O ions. However, for ^7Li , and especially for ^{11}B and ^{12}C ions, the predicted stopping powers are systematically smaller than the experimental values. Again, the ^7Li stopping powers from Z-80 are more closely consistent with the experimental data than stopping powers obtained by the other models.

Comparing the predictions of the models with each other, one may note as a general feature that the scaling of Z-80 predicts lower stopping powers (except in the case of ^{16}O ions in nickel, and ^{16}O and ^{14}N ions in Mylar

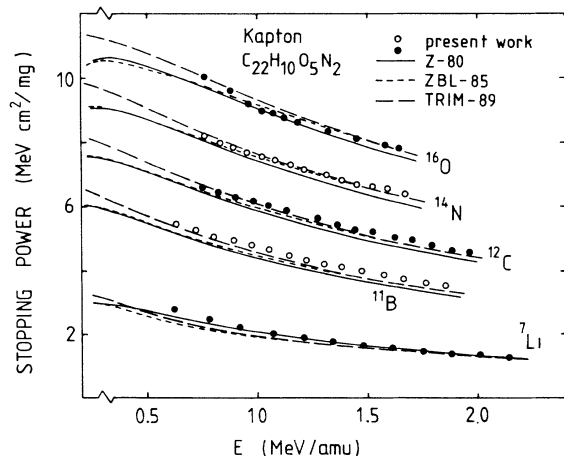


FIG. 3. Stopping powers of Kapton for ^7Li , ^{11}B , ^{12}C , ^{14}N , and ^{16}O ions. Data points and curves are as in Fig. 2.

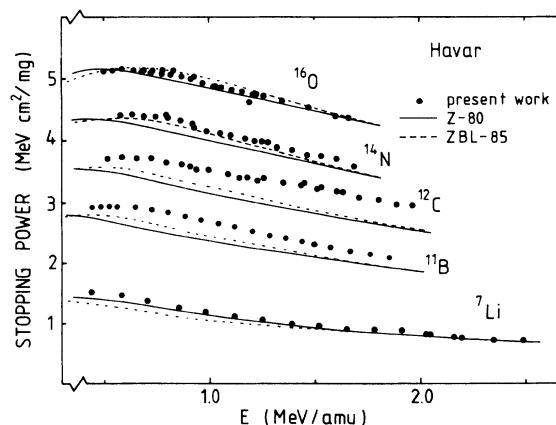


FIG. 4. Stopping powers as in Fig. 3, but for Havar.

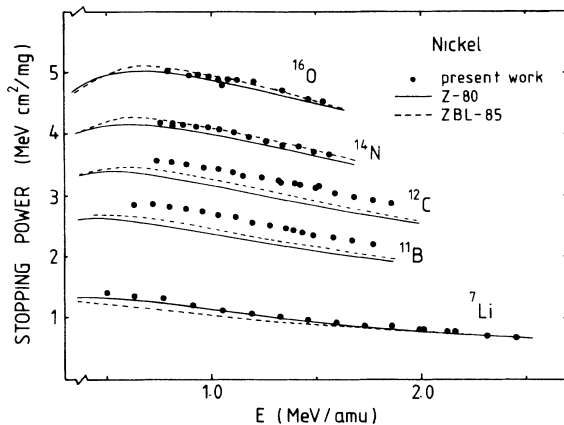


FIG. 5. Stopping powers as in Fig. 3, but for nickel.

below about 1 MeV/amu) than the predictions of ZBL-85 in the present energy region. The TRIM-89 curves exceed the other curves at low energies and fall to the value of the ZBL-85 curves towards the high-energy end of the present energy intervals. For ${}^7\text{Li}$ ions, the systematics for the Z-80 and TRIM-89 curves is different, due to the separate scaling parametrization of the ${}^7\text{Li}$ effective charge.

Our recently obtained experimental stopping data are also comparable with previous experimental values found in the literature. For ${}^7\text{Li}$ and ${}^{12}\text{C}$ ions the data in the literature in the present energy region are surveyed in Refs. 3 and 4. It should be noted that for the composite foil materials no previous data were found.

For ${}^{11}\text{B}$ ions only the stopping powers for nickel may be found in the literature. The data of Roll and Steigert¹³ are derived from energies 2 MeV/amu and higher. The stopping power at the lowest energy point is about 1.8 MeV cm²/mg as obtained from the graph of Ref. 5. This lies about 10% below the value extrapolated from the present data. The data points of Bethge and Sandner^{14,5} (from 5.5 to 22 MeV) lie again systematically well below the calculated curves, the difference being about 20%. The disagreement with the present stopping powers is thus obvious. For ${}^{14}\text{N}$ ions no proper literature values are available and no accurate comparisons may be done as discussed in Ref. 1. For ${}^{16}\text{O}$ ions the present stopping powers in Ni are in excellent agreement with the data of Booth and Grant¹⁵ (in the energy region 2–24 MeV) and with the data of Ward *et al.* (10–67 MeV).¹⁶ The data points in Ni and Havar at the highest ion energy in our previous study were measured by using the method of exposing the foils to a direct beam.² These two data points lie a few percent lower than the present stopping powers, which also agree better with the theoretical predictions.

Some new systematic features in the stopping powers may be observed when all the data are considered together in relation to the semiempirical predictions. Considerations of phenomena such as charge state and sample-foil-thickness dependence of the stopping powers were included in our previous studies.^{2,3}

Significant Z_1 oscillation is evident, especially in the

case of the heavier metallic materials Havar and nickel. For ${}^{14}\text{N}$ and ${}^{16}\text{O}$ ions in these materials the models succeed in predicting the present stopping powers within a few percent, while for ${}^{11}\text{B}$ and ${}^{12}\text{C}$ ions the experimental data exceed the predictions by 15% in the worst case. For ${}^{12}\text{C}$ this is in agreement with Ref. 17 as discussed previously.³ In the light-compound foils of Mylar and Kapton the oscillation is less pronounced.

The fact that the experimental data in comparison with the theoretical approaches show quite similar behavior both for the heavier elemental and composite materials nickel and Havar, may be taken as an indication of the validity of the Bragg's additivity rule. As for the lighter compound materials, Mylar and Kapton, the semiempirical stopping powers again show similar deviations from the experimental data. As no ${}^7\text{Li}$, ${}^{11}\text{B}$, ${}^{12}\text{C}$, ${}^{14}\text{N}$, or ${}^{16}\text{O}$ ion stopping powers exist to our knowledge in solid hydrogen, nitrogen, and oxygen, the deviations can be attributed either to Bragg's rule violations or to the unpredictable heavy-ion stopping powers in these elements.

As indicated in Figs. 2 and 3, the bond corrections applied to the Brandt-Kitagawa theory in TRIM-89 for compounds have their largest effect on the predicted stopping powers near the stopping-power maximum. For ions heavier than carbon these corrections are clearly very successful. In regard to the other two models and the data for Havar and Ni, the predictions of ZBL-85 agree better with the experimental data (except for ${}^7\text{Li}$) than the predictions obtained by the simpler model of Z-80. For the lighter ions, ${}^7\text{Li}$, ${}^{11}\text{B}$, and ${}^{12}\text{C}$, however, even the ZBL-85 model still underestimates the experimental stopping powers.

In regard to ${}^7\text{Li}$ ions, all the models fail seriously for all the materials studied below about 0.5–1.0 MeV/amu. The largest deviations amount to about 15% for Mylar below 0.5 MeV/amu. The fact that the Z-80 model is found to be the most successful in predicting ${}^7\text{Li}$ -ion stopping powers is in good agreement with Lin *et al.*,¹⁸ where ${}^7\text{Li}$ -ion stopping in several elemental target materials are presented. In view of analytical applications, the inability of any of the theoretical approaches to reproduce the stopping powers is most unfortunate, since ${}^7\text{Li}$ ions around 3 MeV are considered as the optimum choice between light and heavy ions in Rutherford-backscattering spectrometry.^{19,20}

Finally, it can be observed that when the stopping-power maxima for the ions $Z < 13$ fall into the present energy interval (${}^{11}\text{B}$, ${}^{12}\text{C}$, ${}^{14}\text{N}$, and ${}^{16}\text{O}$ ions in Havar) the peak generally seems to appear at higher energies than predicted by Z-80. The ZBL-85 predictions are shown to define the maxima more accurately. In the case of ions $Z \geq 13$ in Mylar the Brandt-Kitagawa curves corrected for chemical bonding seem to perfectly reproduce both the position and the height of the stopping peak. Although not plotted for the sake of clarity, the Z-80 scaling model predicts that the lower maxima appear lower in energy for ${}^{27}\text{Al}$ and ${}^{28}\text{Si}$ ions, but higher in energy for ${}^{32}\text{S}$ and ${}^{35}\text{Cl}$ ions, than the maxima in the plotted curves.

To conclude, we present stopping-power and energy-loss data for various ions in some composite materials

and nickel in the energy range 0.2–2.2 MeV/amu. Significant Z_1 oscillations were detected, especially in metallic foils of Havar and Ni, but samples with approximately similar composition showed similar stopping-power behavior. The data are compared with the predictions of semiempirical models. In general, better agreement with the data was observed for the model based on

the Brandt-Kitagawa theory, corrected for the chemical bonding contribution in the case of light compounds of Mylar and Kapton, than for a simpler model based on Z_1 -dependent scaling law. The simpler model is, however, shown to be more consistent with the measured ${}^7\text{Li}$ -ion stopping powers.

-
- ¹J. Räsänen and E. Rauhala, *Phys. Rev. B* **35**, 1426 (1987).
²J. Räsänen and E. Rauhala, *Phys. Rev. B* **36**, 9776 (1987).
³E. Rauhala and J. Räsänen, *Phys. Rev. B* **37**, 9249 (1988).
⁴J. Räsänen and E. Rauhala, *Radiat. Eff. Def. Solids*, **108**, 21 (1989).
⁵J. F. Ziegler, *The Stopping and Ranges of Ions in Matter* (Plenum, New York, 1980), Vol. 5.
⁶W. Brandt and M. Kitagawa, *Phys. Rev. B* **25**, 5631 (1982).
⁷J. F. Ziegler, J. P. Biersack, and U. Littmark, *The Stopping and Ranges of Ions in Matter* (Plenum, New York, 1985), Vol. 1.
⁸J. F. Ziegler and J. P. Biersack, TRIM-89 computer code (private communication).
⁹J. F. Ziegler and J. M. Manoyan, *Nucl. Instrum. Methods* **B35**, 215 (1988).
¹⁰H. H. Andersen and J. F. Ziegler, *Hydrogen Stopping Powers and Ranges in All Elements* (Pergamon, New York, 1977).
¹¹E. Rauhala and J. Räsänen, *Nucl. Instrum. Methods* **B35**, 130 (1988).
¹²D. I. Porat and K. Ramavataram, *Proc. R. Soc. London, Ser. A* **252**, 394 (1959).
¹³P. G. Roll and F. E. Steigert, *Nucl. Phys.* **17**, 54 (1960).
¹⁴K. Bethge and P. Sandner, *Phys. Lett.* **19**, 241 (1965).
¹⁵W. Booth and I. S. Grant, *Nucl. Phys.* **63**, 481 (1965).
¹⁶D. Ward, R. L. Graham, and J. S. Geiger, *Can. J. Phys.* **50**, 2302 (1972).
¹⁷M. Anthony and W. A. Lanford, *Phys. Rev. A* **25**, 1868 (1982).
¹⁸H. H. Lin, L. W. Li, and E. Norbeck, *Nucl. Instrum. Methods* **B17**, 91 (1986).
¹⁹J. P. Thomas, A. Cachard, M. Fallavier, J. Tardy, and S. Marsaud, in *Ion Beam Surface Layer Analysis*, edited by O. Meyer *et al.* (Plenum, New York, 1976), Vol. 1, p. 425.
²⁰E. Rauhala and J. Räsänen, *Nucl. Instrum. Methods* **B35**, 7 (1988).